Cylindrical and Boat-Tailed Afterbodies in Transonic Flow with Gas Ejection

D. M. Sykes*
The City University, London, England

Nomenclature

A = cross-section area of body
b = (subscript) base
C_D = pressure drag coefficient
C_p = pressure coefficient $\{(p - p_\infty)/\frac{1}{2}\rho_\infty U_\infty^2\}$
D = body diameter
I = ejected gas flow parameter $\dot{m}/A\rho_\infty U_\infty$
l = boat-tail length (calibers)
M = Mach number
$\dot{m}$ = mass flow rate
p = pressure
U = velocity
β = boat-tail angle
ρ = density
∞ = (subscript) freestream

1. Introduction

THE base drag of axisymmetric afterbodies may be significantly reduced by ejecting gas at small flow rates into the "dead air" region behind the base[1–4] and also by boat-tailing.[5] The combined effects have been studied at Mach number 2[6] and this Note gives further results for cylindrical afterbodies at Mach numbers from 0.8 to 1.1, and for the combined effects at $M_\infty = 0.95$.

2. Apparatus

The measurements were made in an intermittent ejector driven 9 × 8 in.² perforated wall transonic wind tunnel with atmospheric stagnation pressure and Reynolds number of 4 × 10⁶/ft. The model consisted of a 1 in. diam 5 caliber centerbody and interchangeable 2 caliber afterbodies. The centerbody was supported on a pair of 45° swept forward hollow struts (see Fig. 1a), one strut contained pressure tubes

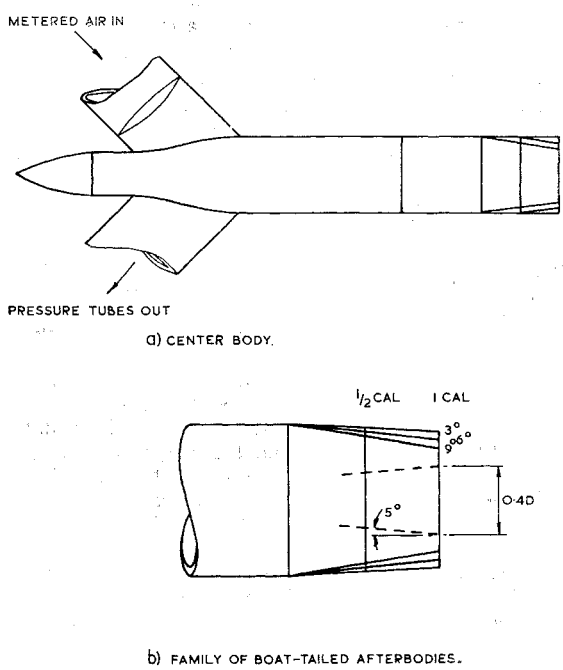

Fig. 1 Diagram of models.

Received July 7, 1969; revision received November 17, 1969. This work was supported by the British Ministry of Defence.
* Lecturer in Department of Aeronautics.

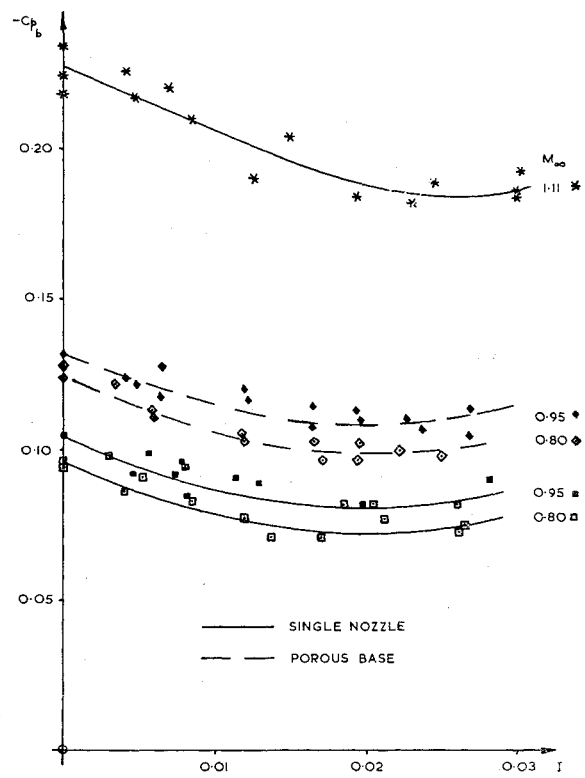

Fig. 2 Cylinder base pressure.

and the other supplied the metered air for ejection. The centerbody-strut intersection was profiled by simple sonic area rule to give constant normal cross-section area of body and struts equal to that of the cylindrical centerbody. The body extended forward for ½ caliber as a cylinder carrying a boundary layer transition strip, and was capped with a 2 caliber ogive nose. Since the boundary layer was turbulent and the trailing edge of the struts was 4 calibers ahead of the base, the base pressures were unlikely to suffer from support

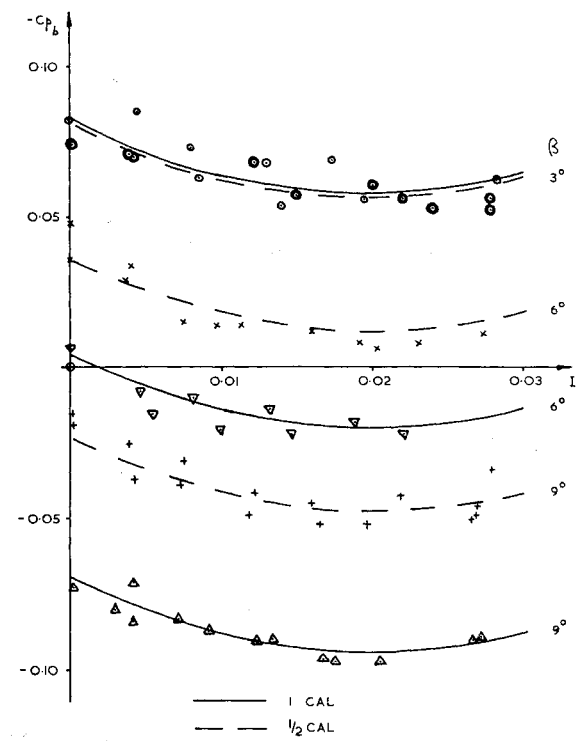

Fig. 3 Boat-tail base pressure.

interference.[7] The afterbodies consisted of a cylinder and six conical boat-tails with angles 3°, 6°, and 9° and of lengths $\frac{1}{2}$ and 1 caliber, each contained a nozzle of 0.4 caliber exit diam (see Fig. 1b). Previous tests[2-4] in supersonic streams have shown that the nozzle geometry has little effect on base pressure at low ejected flow rates.

3. Results

The boundary layer near the base of the model was investigated at $M_\infty = 0.99$; the thickness was close to that predicted for a fully turbulent layer and the velocity distribution conformed to a $\frac{1}{7}$th power law profile. The ratio of boundary layer thickness to model diameter was $\frac{1}{8}$, which is typical of conventional projectiles.

Pressure distribution over a cylindrical model base without a nozzle was measured at $M_\infty = 0.80$, 0.95, and 1.11. The pressure coefficient on the base with a nozzle and on the afterbody $\frac{1}{2}$ caliber upstream was measured as a function of the ejected flow parameter I at the same Mach numbers. The pressures on the afterbody were almost independent of I, while the base pressure coefficients varied as shown in Fig. 2. The values of C_{p_b} at $I = 0$ were all slightly smaller than those measured on the base without a nozzle.

Also shown in Fig. 2 is the dependence of C_{p_b} on I at $M_\infty = 0.80$ and 0.95 for a cylindrical afterbody with a porous base used by Bowman and Clayden.[3] Unlike their experiments, the present results showed little change in the behavior of C_{p_b} with I for this change of base design; the values of C_{p_b} at $I = 0$ were in close agreement with those measured on the base without a nozzle.

The pressure distribution on the boat-tailed afterbodies was measured at $M_\infty = 0.95$. The flow was found to go supersonic over the shoulder at the start of the boat-tail, but underwent rapid compression about $\frac{1}{4}$ caliber downstream of this shoulder, followed by slow subsonic compression. Schlieren photographs showed that the flow was attached to the boat-tail surface throughout. Pressures on the boat-tail and cylindrical afterbody were independent of ejected mass flow rate. The result for base pressure coefficient as a function of I for the family of boat-tails is shown in Fig. 3. It appeared that at this Mach number the base pressure could

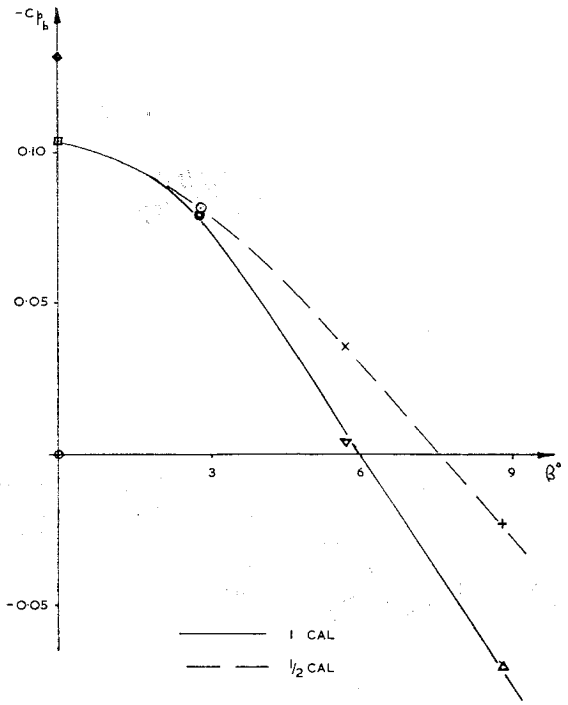

Fig. 4 Boat-tail angle and base pressure.

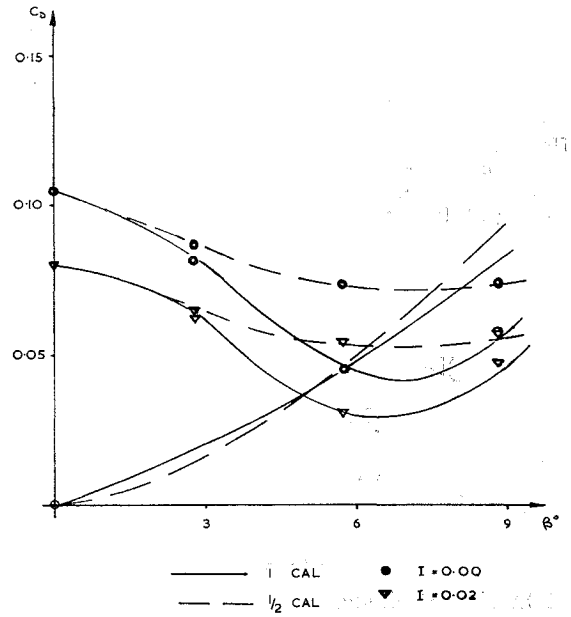

Fig. 5 Boat-tail and afterbody drag coefficient.

be written as

$$C_p = C_{p_b}(\beta,l)_{I=0} + C_{p_b}(I)$$

The best fit quadratic for the latter term was found as

$$C_{p_b}(I) = -2.4I + 60I^2$$

for $I \leqslant 0.03$ and is shown in the curves in Fig. 3. This curve is shown fitting the data in Fig. 2 for both solid and porous base cylinders at $M_\infty = 0.80$ and 0.95, but not for $M_\infty = 1.11$. The values of $(C_{p_b})_{I=0}$ at $M_\infty = 0.95$ were also determined in this analysis and are shown in Fig. 4, plotted against boat-tail angle β for the two afterbody lengths. For both boat-tail lengths at $\beta = 9°$ measured base pressures were higher than freestream static, the longer boat-tail producing greater pressure recovery.

Afterbody pressures were integrated to give boat-tail drag coefficients, and combined with base pressures, assumed to be constant over the base and exit of the nozzle, to give afterbody drag coefficients C_D. These results are shown in Fig. 5, which also shows the effect of drag reduction by gas ejection at the optimum rate $I = 0.02$. The effect of thrust from ejected gas momentum has not been included; this could amount to about 0.02 change in C_D at $I = 0.03$. The results show that the optimum boat-tail angle (of about 7°) is relatively insensitive to gas ejection rate or boat-tail length. The same optimum condition and behavior were found by Bowman and Clayden[6] at $M_\infty = 2.0$.

References

[1] Cortright, E. M. Jr. and Schroeder, A. H., "Preliminary Investigation of Effectiveness of Base Bleed in Reducing Drag of Blunt Base Bodies in Supersonic Stream," RM E51 A26, 1951, NACA.

[2] Reid, J. and Hastings, R. C., "The Effect of a Central Jet on the Base Pressure of a Cylindrical Afterbody in a Supersonic Stream," RM 3224, 1961, Aeronautical Research Council.

[3] Bowman, J. E. and Clayden, W. A., "Cylindrical Afterbodies in Supersonic Flow with Gas Ejection," *AIAA Journal*, Vol. 5, No. 8, 1967, pp. 1524–1525.

[4] Harries, M. H., "Pressure on Axisymmetric Base in a Transonic or Supersonic Free Stream in the Presence of a Jet," Rept. 111, 1967, FFA.

[5] McDonald, H. and Hughes, P. F., "Correlation of High Subsonic Afterbody Drag in the Presence of a Propulsive Jet or

Support Sting," *Journal of Aircraft*, Vol. 2, No. 3, 1965, pp. 202–207.

[6] Bowman, J. E. and Clayden, W. A., "Boat-Tailed Afterbodies at $M = 2$ with Gas Ejection," *AIAA Journal*, Vol. 6, No. 10, Oct. 1968, pp. 2029–2030.

[7] Heyser, A., Maurer, F., and Oberdörffer, E., "Experimental Investigation on the Effect of Tail Surfaces and Angle of Attack on Base Pressure in Supersonic Flow," AGARD Conference Proceeding 10, 1966, pp. 267–290.

Electric Arc Moving at Hypersonic Speed

JAN ROSCISZEWSKI*
Air Vehicle Corporation, San Diego, Calif.

1. Introduction

EKDAHL, Kribel, and Lovberg[1] experimentally observed a rotating spoke in an MPD arc jet in argon. The velocity of the rotation corresponds to the hypersonic Mach number of around 30 based on the speed of sound at cold flow.

As is indicated at the end of this paper, calculations based on Lovberg's experimental data indicate that the arc could behave like a solid body at hypersonic speed. This is similar to the case of arcs moving at subsonic speed as indicated by some authors.[2,3]

In the present paper, using a Newtonian pressure distribution corresponding to a thin shock layer at hypersonic speed, the shape of the arc is derived. It is assumed that the electric field and temperature are constant in the arc cross section. The last assumption is justified because the plasma is fully ionized within the spoke. A high electron conductivity results in a nearly constant temperature. Indeed, recent experiments have supported this assumption, indicating measured temperature surprisingly constant and equal about 1 ev.[4] The spoke is driving an ionizing shock wave (Fig. 1). The plasma in the thin shock layer is a source of strong line radiation.

2. Derivation of the Shape of an Arc

We shall assume a uniform applied magnetic field B and a small induced field. Conservation of momentum in the x direction gives

$$\partial p/\partial x = jB = \sigma(E - U_\infty B)B \tag{1}$$

$$\partial p/\partial y = 0 \tag{2}$$

The electric conductivity is given by the Spitzer formula (MKS units)

$$\sigma = \frac{1.5 \times 10^{-2} T^{3/2}}{\ln[1.23 \times 10^7 (T^{3/2}/n_e^{1/2})]} \tag{3}$$

with

$$p = knT \tag{4}$$

one obtains from Eq. (1)

$$dknT/dx = \sigma(n,T)(E - U_\infty B)B \tag{5}$$

Assuming fully ionized gas ($n = 2n_e$) within the spoke, and $T = \text{const}$, one obtains

$$kT \int \frac{dn}{\sigma(n)} = (E - U_\infty B)Bx \tag{6}$$

or taking into account relation in (3), the preceding integral can be calculated as follows:

$$\int \frac{\ln[1.23 \times 10^7 (T^{3/2}/n_e^{1/2})]dn}{1.51 \times 10^{-2} T^{3/2}} = \frac{n\{\ln[1.23 \times 10^7 T^{3/2}/(\frac{1}{2}n)^{1/2}]\}}{1.51 \times 10^{-2} T^{3/2}} + C$$

Noting that $\ln(n^{1/2})$ is a slow function of n, the expression in parenthesis can be taken as constant. This is equivalent to the constant current density throughout the arc. Therefore,

$$\int \frac{dn}{\sigma(n)} = K_1 n + C$$

where

$$K_1 = \frac{\ln\{[1.23 \times 10^7 T^{3/2}/(\frac{1}{2}n)^{1/2}]\} + 1}{1.51 \times 10^{-2} T^{3/2}}$$

Taking into account that E and B are constant, one obtains from Eqs. (6) and (4)

$$p = K_2 x + C_1 \tag{7}$$

where

$$K_2 = \frac{(E - U_\infty B)B}{K_1}$$

The constant C_1 can be calculated by equating the pressure from Eq. (7) with the Newtonian stagnation point pressure $p_s = \rho_\infty U_\infty^2$ at $x = x_m$ (Fig. 1).

Therefore,

$$C_1 = \rho_\infty U_\infty^2 - K_2 x_m \tag{8}$$

denoting

$$\bar{p} = \frac{p}{\rho U_\infty^2}, \quad \bar{x} = \frac{K_2 x}{\rho_\infty U_\infty^2}, \quad \bar{y} = \frac{K_2 y}{\rho_\infty U_\infty^2} \tag{9}$$

one obtains

$$\bar{p} = 1 - (\bar{x}_m - \bar{x}) \tag{10}$$

Assuming a Newtonian pressure distribution over a solid body, i.e.,

$$\bar{p} = \cos\alpha = \frac{[d\bar{y}/d\bar{x}]^2}{1 + [d\bar{y}/d\bar{x}]^2} \tag{11}$$

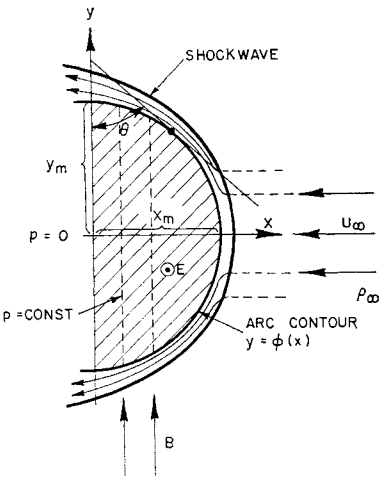

Fig. 1 Arc cross section in hypersonic flow.

Received February 13, 1969; revision received December 1, 1969. This paper has been supported by the Air Force Office of Scientific Research Contract F44620-68-C-0052. The author wishes to express his appreciation for the many fruitful discussions with R. Lovberg and R. Dethlefsen.

* Consultant.